Numerical Simulations of Wake Flows of Floating Offshore Wind Turbines by Unsteady Actuator Line Model

Pengfei Li[1,2], Ping Cheng[1,2], Decheng Wan[1,2*] and Qing Xiao[3]

1. State Key Laboratory of Ocean Engineering, School of Naval Architecture, Ocean and Civil Engineering, Shanghai Jiao Tong University,
2. Collaborative Innovation Center for Advanced Ship and Deep-Sea Exploration, Shanghai 200240, China
3. Department of Naval Architecture, Ocean and Marine Engineering, University of Strathclyde, UK
*Corresponding author: dcwan@sjtu.edu.cn

Abstract: The aerodynamic performance of the offshore wind turbines on floating platforms differ from that on bottom-fixed platforms because of the unsteady character caused by its supporting platform motions. Nowadays several floating offshore wind turbine (FOWT) programs have been in trial operation in some areas, but the unsteady aerodynamics of FOWT is still not adequately studied owing to the lack of effective unsteady modelling methods. In this paper, an unsteady actuator line model coupled with three-dimensional Reynolds Averaged Navier-Stokes Equations was developed to numerically simulate of wake flows of the floating wind turbine experiencing periodical surge and pitch motions. The simulation is first conducted without effects of platform motions, and the results are compared with other approaches from previous studies. Then the effects of platform surge and pitch motions with typical angular frequencies on the integrated loads and wake character are investigated. The analysis of results shows that the typical surge motions are sufficiently slow having small influence on the integrated loads while the typical pitch motions have significant effects on the aerodynamic performance of the FOWT.

Keywords: unsteady aerodynamics, FOWT, surge and pitch, actuator line model, platform motions

1 Introduction

The concept of floating offshore wind turbine (FOWT) system has been proposed for around 30 years. But the first installation of FOWT in deep water was implemented only several years ago. Today, most of the offshore wind turbine are installed in shallow water. However, areas of deep water have much stronger and steadier wind resource. Some previous feasibility and economy research indicates that floating platforms are economically viable solution in the sea area with depth more than 50 meters. Although several floating wind turbine systems such as Hywind (Norway) and Blue (Italy) are in trial operation worldwide, the unsteady aerodynamic performance of FOWT experiencing platform motion are still not studied adequately. Traditionally, analysis codes (e.g. FAST and HAWC2) used to calculating the experienced loads on floating wind turbine structures all base aerodynamic computation on blade element momentum (BEM) theory. The BEM method takes the unsteady effects into account by including ad hoc formulations such as dynamic inflow model, yaw/tilt model. The additional degrees of freedom (DoFs) imposed on the floating foundations results in the highly unsteady properties of the floating wind turbine aerodynamics. Due to the additional wind velocity component, a floating supporting structure of offshore wind turbine may lead to the violation of the fundamental momentum balance assumptions that underlie those common used methods. Reduced frequency analysis presented by Sebastian (2013) has indicated that the flow type of most floating wind turbines is unsteady or highly unsteady. These factors have given rise to the necessities for more accurate and more advanced methods to simulate the unsteady aerodynamics of the wind turbine mounted on the floating structure.

Studies focused on the unsteady aerodynamics of the floating wind turbines renders some discrepancies on thrust and power, etc. By using the overset mesh technique in Star-CCM+, Tran, et al (2014) illustrate the unsteady aerodynamics of a floating offshore wind turbine experiencing the prescribed pitching motion of the floating platform as a sine function. He gave an astonishing result which indicates that the thrust increases by approximately 30% for a 4° amplitude pitch motion while the aerodynamic power increased by 100%. Guo Zhenxiang (2013) conducted a simulation with the free itching motion which illustrated that the averaged power decreased by 1~2% with an averaged pitch angle of 5 degree. J. B. de Vaal, et al (2014) also presented a similar reduction of thrust, using a moving actuator disc model. Other example of the modeling of aerodynamic force on a floating wind turbine, using a wide range of methods, gives quite different results.

Foundation item: Supported by National Natural Science Foundation of China (Grant Nos. 51379125, 51490675, 11432009, 51411130131)
***Corresponding author Email:** dcwan@sjtu.edu.cn

In this work, the unsteady aerodynamic forces and wake flows of a wind turbine with the supporting platform surging and pitching as a sine motion are investigated. By virtue of the platform motions, the wind turbine rotor will be moving into and out of its own wake. An unsteady actuator line model are used to investigate the forces and simulate the wake fields. The steady actuator line model will be verified first for its ability to simulate the aerodynamic performance of the wind turbines. All the simulations and code development are conducted on the open source software OpenFOAM.

2 Actuator Line Model

The actuator line model (ALM) provides a means of effectively displacing the real blade surfaces with virtual actuator lines, in consequence, has a benefit of not requiring to solve the blade geometry layer. This is accomplished by discretized the blades into span-wise sections of constant airfoil, chord, twist and distributing the forces over them.

2.1 Basic principles

In this aerodynamic model, a three-dimensional Navier-Stokes solver is combined with a so-called actuator line technique in which body forces are distributed along rotating lines. Full three-dimensional Navier–Stokes simulations thus govern the flow field, whereas the loads on each blade are determined from the local angle of attack and tabulated airfoil data. The basic incompressible Navier–Stokes equations underpin the model is:

$$\nabla \cdot \mathbf{U} = 0,$$
$$\frac{\partial \mathbf{U}}{\partial t} + \mathbf{U} \cdot \nabla \mathbf{U} = -\frac{1}{\rho}\nabla p + \nu \cdot \nabla^2 \mathbf{U} + \frac{1}{\rho}\mathbf{f}_\varepsilon \quad (1)$$

where $\mathbf{f}_\varepsilon$ denotes the body forces, which representing the loads on the rotating blades. The body forces acting on the blades are determined using a blade element approach combined with two-dimensional airfoil characteristics. For every blade element, the relative velocity, $\overrightarrow{U_{rel}}$, and flow angle, φ, with respect to rotor plane are determined as follows.

$$\overrightarrow{U_{rel}} = \overrightarrow{U_{in}} + \overrightarrow{U_{rot}} \quad (2)$$

$$\varphi = \arcsin\left(\frac{U_{rel,z}}{\left|\overrightarrow{U_{ref}}\right|}\right) \quad (3)$$

The lift and drag per span-wise length are calculated once the local angle of attack is given by α=φ-γ, where γ denotes the local pitch angle.

$$\mathbf{f} = \frac{d\mathbf{F}}{rdrd\theta dz} = \frac{\rho U_{rel}^2 c N_b}{2rdrd\theta dz}\left(C_L \overrightarrow{e_L} + C_D \overrightarrow{e_D}\right) \quad (4)$$

Where C_L and C_D are two-dimensional airfoil lift and drag coefficients, which are determined by lookup table. The applied aerodynamic blade forces need to be distributed smoothly on several mesh points in order to avoid singular behavior. In practice, a 3D Gaussian correction is made to smooth the force out over the blade by taking the convolution of the force with a regularization kernel, $\mathbf{f}_\varepsilon = \mathbf{f} \otimes \eta_\varepsilon$, where

$$\eta_\varepsilon(d) = \frac{1}{\varepsilon^2 \pi^{3/2}} \exp\left[-\left(\frac{d}{\varepsilon}\right)^2\right] \quad (5)$$

Here, *d* is the distance between cell-centered grid points and the i'th actuator line point, and ε is parameter that serves to adjust the concentration of the regularized loads. Hence, the body forces projected to the flow field per unit volume becomes:

$$\mathbf{f}_{\varepsilon,i}(x,y,z,t) = -\sum_{j=1}^{N} \mathbf{f}_i\left(x_j, y_j, z_j, t\right) \frac{1}{\varepsilon^3 \pi^{3/2}} \exp\left[-\left(\frac{d_j}{\varepsilon}\right)^2\right] \quad (6)$$

2.2 Unsteady actuator line model

Modifications to the standard actuator line model have to be made to be capable of simulating a wind turbine rotor oscillating in surge and pitch motions. Starting at an initial position, located at the origin *x=0*, the position of actuator line without consideration of blade rotating is updated at the end of each time step, as $x(t) = x_A \sin(\omega t)$. The updated position is then added to the rotating displacement to determine the index of the grid cells in which the actuator line points are located. Fluid velocities at the actuator line points' location and the moving velocities imposed by the periodic motion need to be sampled to evaluate equations (2)-(4), which determine the volume forces that applied to the flow field in the next time step. Once the loading on the actuator lines themselves has been updated, the Gaussian smearing function, (5), is used to the corresponding volume force that should be applied to each cell in the computational grid.

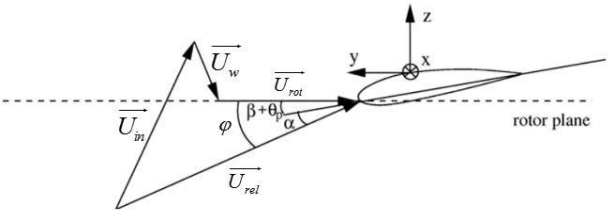

Fig.1 Velocity triangle seen locally on a blade section

To find the relative velocity seen by the blade, $\overrightarrow{U_{rel}}$, the rotational velocity, $\overrightarrow{U_{rot}}$, plus the surging or pitching velocity, $\overrightarrow{U_w}$, must be added as vectors to incoming wind velocity $\overrightarrow{U_{in}}$ as shown in Figure 1(Hansen, 2013).

$$\overrightarrow{U_{rel}} = \overrightarrow{U_{in}} + \overrightarrow{U_{rot}} + \overrightarrow{U_w} \quad (7)$$

3 Simulation Setup

In this study, the well-known NREL 5MW baseline wind turbine (see Butterfield, 2007) has been considered for numerical simulations. Table 1 shows the overall specifications of the NREL 5MW baseline wind turbine. The cross sections of rotor blade consist of series of DU (Delft University) and NACA 64xxx airfoils from the hub to the

outboard section. Related aerofoil data can be found from Bazilevs et al (2011). Note that the blade pitch is designed to be zero at rated situation and varies with incoming wind speed.

Table 1. Depiction of NREL 5MW baseline wind turbine

Rating	5MW
Rotor Orientation	Upwind
Number of Blades	3
Rotor, Hub Diameter	126, 3m
Hub Height	90m
Cut-in, Rated, Cut-out Wind Speed	3m/s, 11.4m/s,25m/s
Cut-in, Rated Rotating Speed	6.9rpm, 12.1rpm
Overhang, Shaft tilt, Precone Angles	5m, 5deg, 2.5deg

3.1 Verification of baseline cases

In order to show some comparison results for the present aerodynamic method, the baseline cases without platform motions has been considered first. Figure 2 shows the comparison results for the verification of the steady aerodynamic analysis for different wind speed. The present study by actuator line model shows good agreement with the previous results by Thanh-Toan et al. using FLUENT and Chow et al. using OVERFLOW2. Additionally, Jonkman's results using FAST BEM with consideration of dynamic stall model are also compared. The aerodynamic forces of steady cases considering tilt and precone angles show very good agreement with that by previous studies. That gives us confidence to extend this model to modelling the unsteady aerodynamics of wind turbines with platform surge or pitch motions.

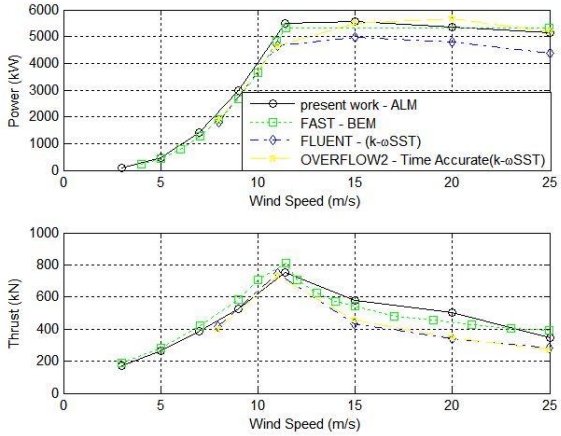

Fig.2 Comparison of predicted aerodynamic loads for various wind speed

3.2 Setup of unsteady cases

The unsteady actuator line model presented in section 2.2 is used in subsequent work that simulate the rotor aerodynamics with the platform surge and pitch motion attached. The code development of unsteady actuator line model is based on the open source CFD tool, OpenFOAM. This model can be included by any incompressible fluid solver as a dynamic-linked C++ class library.

3.2.1 Parameters for surge and pitch motions

Table 2. Operating conditions for unsteady simulations

Parameter	Value
Wind speed, V_0	11.4m/s
Rotating speed, Ω	1.2671rad/s
Blade pitch, θ_0	0.0°
Surge frequency, ω_s	0.246rad/s
Amplitude of surge motion	4, 8, 16m
pitch frequency, ω_p	0.314rad/s
Amplitude of pitch motion	2°, 4°, 8°

The surge and pitch motions experienced by the rotor of a floating offshore wind turbine are greatly depended on the type of supporting foundation and the dominating sea state. We don't care about the mechanisms that generate the surge and pitch motions but focus on the reasonable values of those motions. To ensure that a realistic range of values are considered, values for surge motion frequency and amplitude are obtained from a conceptual study (Wayman, et al., 2006) performed for NREL 5MW wind turbine mounted on substructures developed by NREL. The frequency of pitch motion is selected by referring to the common pitching frequencies of semi-submersible platforms. The operating conditions for the unsteady actuator line simulations are listed in Table 2. The simulations run under the constant surge or pitch frequency with the amplitude varying.

3.2.2 Outlines of simulation approach

To avoid numerical instability, the additional platform motion is set to zero in the beginning and the oscillating starts after hundreds of time steps. All simulations start off with a stationary rotor located at the origin, operating in a steady wind, with fixed rotating speed and blade pitch settings as given in Table 2. For the first 15s of the simulations, this maintained. Thereafter, the surge or pitch oscillations are started. At least 4 full cycles are completed before ending the simulations to ensure that all start-up transients have been eliminated. As a representative cycle, data from the last complete oscillation period are extracted for analyses. Furthermore, comparisons at fixed time intervals during a representative cycle (namely 0T, 0.25T, 0.5T and 0.75T) are also made.

The computational grid used for all calculations with the unsteady actuator line model are described in Figure 3, which extends 4D upstream and 9D downstream in the axial direction from the neutral position of the rotor plane, and 4.5D in the lateral direction from the rotor axis. The axial inflow velocity is prescribed on the inlet boundary, and a zero gradient pressure condition is defined on the outlet boundary, with a symmetry boundary condition on the lateral boundary. Following experiences provided by Nodeland (2013), the

Gaussian smearing parameter is set to $\varepsilon = 2\Delta x$ (Δx is the minimal, axial length of grid cell), and the time step is selected to ensure that the actuator line spins across no more than one grid cell. In this paper, a time step of $\Delta t = 0.02s$ is used throughout.

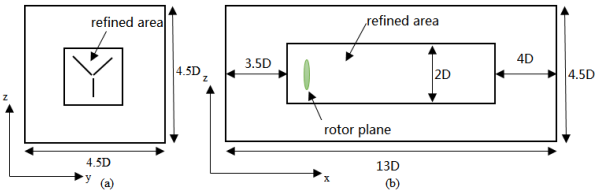

Fig.3 Sketch of computational domain

4 Results and Discussion

4.1 Aerodynamic loads

The aerodynamic loads of the floating wind turbine experiencing additional surge motion is shown in Figure 4(a)-(c), while that experiencing pitch motion is shown in Figure 4(d)-(f). As illustrated in the former three figures, the aerodynamic loads are becoming more and more unsteady with the increase of surge amplitude. It's a striking phenomenon that enormous steep rise and fall emerge during the surge processing, which will hugely impact the fatigue performance and strength safety of the structure. Hence, measures should be taken to prohibit the platform from surge motion of great amplitude.

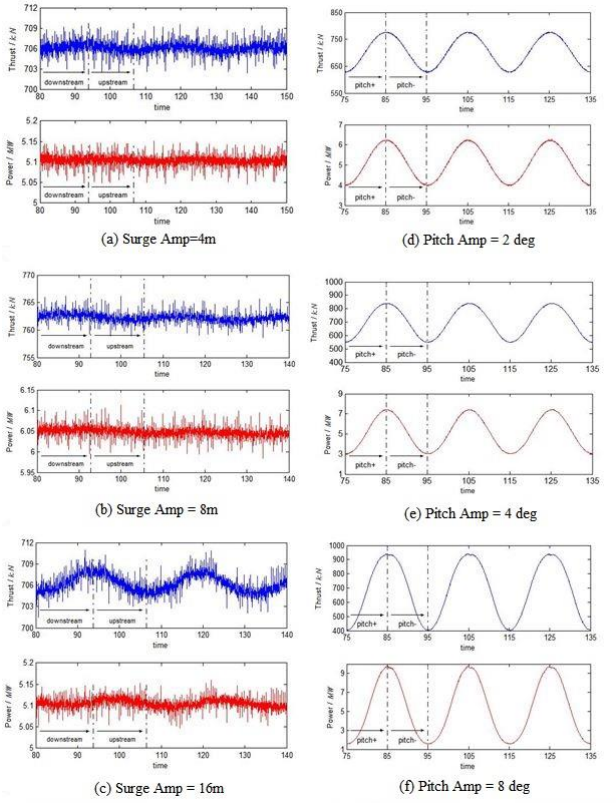

Fig.4. Unsteady aerodynamic loads at the final three cycles for rotor experiencing surge or pitch motion

In figure 4(d)-(f), the upper of the rotor moves into its wake in the first 10 seconds and then it pitches reversely. It's observed that the variation of aerodynamic loads presents an obvious law, similar to a sine function. With the increasing of pitch amplitude, the fluctuating extent becomes larger. This type of fluctuation will lead to that loads acting on the blades varies for loops. The high peaks of thrust and power cause by platform pitching motion indicates that more advanced controlling system should be designed to eliminate the emergence of these huge loads.

The averaged thrust and power calculated from the last steady cycle are given in Table 3 and Table 4. Referentially, the averaged aerodynamic thrust and power are 714.3kN, 5.206MW respectively without consideration of surge motion. Compared to the corresponding steady values, the averaged aerodynamic forces with different amplitudes of surge motion are a little lower. That decrease indicates that the platform surge motion will trigger the reduction of power harvested from the wind. The reduction of power or thrust will rise if the surge amplitude increases. It's weird that the aerodynamic power has a slight increase when the pitching amplitude is equal to 8°. The reason for that is hard to imagine.

Table 3. Averaged aerodynamic forces with different amplitude of surge motion

Amplitude (m)	Power (MW)	Thrust (kN)
4	5.113	706.7
8	5.107	706.3
16	5.103	705.8

Table 4. Averaged aerodynamic forces with different amplitude of pitch motion

Amplitude (deg)	Power (MW)	Thrust (kN)
2	5.110	704.1
4	5.156	699.9
8	5.365	687.0

4.2 Wake flows

The evolution of wake vortex at the representative cycle (namely 0T, 0.25T, 0.5T and 0.75T) for different surging and pitching motion is illustrated in Figure 5-10. The wake vortex was visualized by the second-order invariant of velocity gradient, e.g. Q in OpenFOAM (see Digraskar, 2010). The contours of Q gives a visual representation of the wake behind the rotor. In Figures 5-10, the instantaneous vorticity distribution at the start of an oscillation cycle is shown in subgraph (a), whereas that at the other three typical time are shown subsequently. For different oscillation amplitude, there is a slight increase in wake expansion visible near the rotor. The wake structure downstream the rotor is also more affected by the time varying loads on the rotor due to the oscillations. Because of the rotor motion, a discontinuity downstream the rotor plane, which is not apparent with the surge motion and is very clear and outstanding with the pitch motion, appears at each graph of different time.

In Figures 5-7, for the lowest surging amplitude, the root and tip vortices closely resemble those for a stationary rotor, with slight deviations in the wake only visible approximately half rotor radius downstream. With the rotor moving into and out of its wake flows, the screw pitch of this type of spiral wake has a snap increasing after about half rotor radius.

By contrast, the root and tip vortices for any pitching amplitude, shown in Figures 8-10, are very different from that for a stationary rotor. The wake vortex is highly unsteady because of the pitching motion, which indicates that the platform pitching motion has great influence on the wake flows of a floating wind turbine rotor. As illustrated in a full cycle of wake development for pitching motion, the wake vortex near the rotor plane has an axial velocity with the same phase as the pitching motion while the wake vortex in the far field has a reverse axial velocity. The paired vortex rings oriented towards different axial direction emerges about two radii behind the rotor. At the highest pitching amplitude considered, the wake vortex structures in Figure 10 differ significantly from those observed at the lower pitching amplitudes.

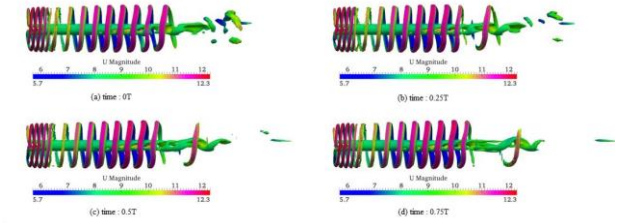

Fig.5 wake vortex visualization: surge amplitude=4m

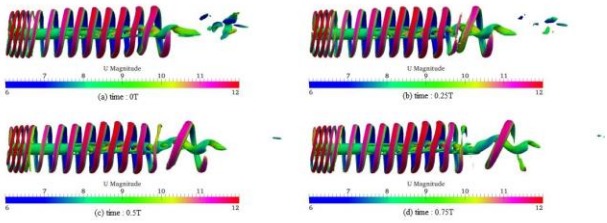

Fig.6 wake vortex visualization: surge amplitude=8m

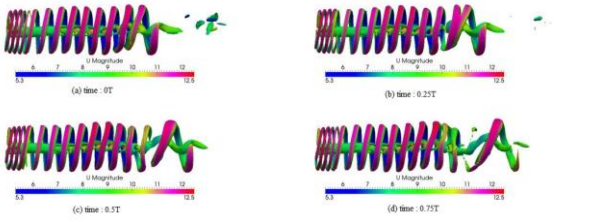

Fig.7 wake vortex visualization: surge amplitude=16m

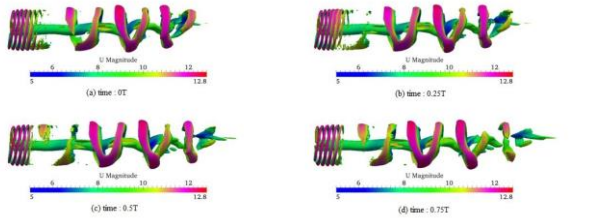

Fig.8 wake vortex visualization: pitch amplitude=2 °

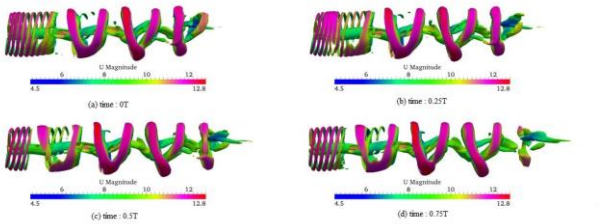

Fig.9 wake vortex visualization: pitch amplitude=4 °

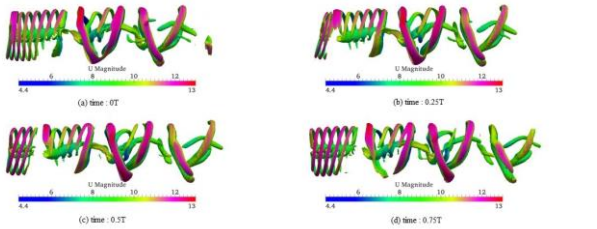

Fig.10 wake vortex visualization: pitch amplitude=8 °

5 Conclusions

The aerodynamic loads acting on the floating foundations dramatically reduce the stiffness of the tower and supporting structure. In contrast to the equivalent bottom fixed system, larger system motions can be expected on the floating wind turbine system. In this study, a complex unsteady aerodynamic analysis on rotating rotor blades of a floating supporting system experiencing surge and pitch motions has been successfully conducted using unsteady actuator line model. This unsteady model is time-accurate and fully three dimensional.

It seems that the platform surging motion has modest influence on the aerodynamic forces and wake flows of a rotor. In contrast, the pitching motion has greater impact on aerodynamic loads and wake flows of the rotor. From the simulation results, especially for the pitching motion, the wake geometry does not exactly resemble the idealized Joukowsky wake depicted by momentum theory. These differences are significant enough for causing the BEM theory-based models to fail if the floating system experiences a large pitching motion.

Surge and pitch motion are only two of six possible degrees of freedom for a floating system. It could be useful to further study the effects of other type of motions, such as yaw and heave. For a step further, we can also research the impacts on the rotor aerodynamics caused by surge and pitch motions with different frequencies. We also plan to coupled the unsteady ALM with our research group's inhouse hydrodynamic solver naoeFoam-SJTU. This full coupled turbine-floater-tether model is ongoing, and may contribute to the research of turbine-floater interactions.

Acknowledgement

This work is supported by National Natural Science

Foundation of China (Grant Nos. 51379125, 51490675, 11432009, 51411130131), The National Key Basic Research Development Plan (973 Plan) Project of China (Grant No. 2013CB036103), High Technology of Marine Research Project of The Ministry of Industry and Information Technology of China, Chang Jiang Scholars Program (Grant No. T2014099) and the Program for Professor of Special Appointment (Eastern Scholar) at Shanghai Institutions of Higher Learning (Grant No. 2013022), to which the authors are most grateful.

References

Sebastian, T., & Lackner, M. A. (2013). Characterization of the unsteady aerodynamics of offshore floating wind turbines. *Wind Energy*, *16*(3), 339-352.

Tran, T., Kim, D., & Song, J. (2014). Computational Fluid Dynamic Analysis of a Floating Offshore Wind Turbine Experiencing Platform Pitching Motion. *Energies*,*7*(8), 5011-5026.

Vaal, J. D., Hansen, M. O., & Moan, T. (2014). Effect of wind turbine surge motion on rotor thrust and induced velocity. *Wind Energy*, *17*(1), 105-121.

Thanh-Toan Tran et al. (2013). Extreme Load Estimation for a Large Wind Turbine Using CFD and Unsteady BEM

Chow, R., & Van Dam, C. P. (2011, January). Inboard stall and separation mitigation techniques on wind turbine rotors. In *Proceedings of 49th AIAA Aerospace Sciences Meeting, Orlando, FL, USA* (pp. 4-7).

Bazilevs, Y., Hsu, M. C., Akkerman, I., Wright, S., Takizawa, K., Henicke, B., ... & Tezduyar, T. E. (2011). 3D simulation of wind turbine rotors at full scale. Part I: Geometry modeling and aerodynamics. International Journal for Numerical Methods in Fluids, 65(1‐3), 207-235.

Bazilevs, Y., Hsu, M. C., Kiendl, J., Wüchner, R., & Bletzinger, K. U. (2011). 3D simulation of wind turbine rotors at full scale. Part II: Fluid–structure interaction modeling with composite blades. International Journal for Numerical Methods in Fluids, 65(1‐3), 236-253.

Wayman, E. N. (2006). *Coupled dynamics and economic analysis of floating wind turbine systems* (Doctoral dissertation, Massachusetts Institute of Technology).

Nodeland, A. M. I. (2013). *Wake Modelling using an actuator disk model in openFOAM*. Ph.D. thesis, Norwegain University of Science and Technology, 100-127.

Hansen, M. O. (2013). *Aerodynamics of wind turbines*. Routledge, Denmark, 76.

Butterfield, S., Musial, W., & Scott, G. (2009). *Definition of a 5-MW reference wind turbine for offshore system development*. Golden, CO: National Renewable Energy Laboratory.

Shives, M., & Crawford, C. (2013). Mesh and load distribution requirements for actuator line CFD simulations. *Wind Energy*, *16*(8), 1183-1196.

Peet, Y., Fischer, P., Conzelmann, G., & Kotamarthi, V. (2013). Actuator Line Aerodynamics Model with Spectral Elements. In *51st AIAA Aerospace Sciences Meeting including the New Horizons Forum and Aerospace Exposition*.

Jeon, M., Lee, S., & Lee, S. (2014). Unsteady aerodynamics of offshore floating wind turbines in platform pitching motion using vortex lattice method. *Renewable Energy*, *65*, 207-212.

Digraskar, D. A. (2010). *Simulations of flow over wind turbines*. Master thesis, University of Massachusetts, 60-61.